Microbes Environ. Vol. 34, No. 3, 278-292, 2019
https://www.jstage.jst.go.jp/browse/jsme2 doi:10.1264/jsme2.ME19017

Geochemical and Metagenomic Characterization of Jinata Onsen, a Proterozoic-Analog Hot Spring, Reveals Novel Microbial Diversity including Iron-Tolerant Phototrophs and Thermophilic Lithotrophs

Lewis M. Ward[1,2,3]*, Airi Idei[4], Mayuko Nakagawa[2], Yuichiro Ueno[2,5,6], Woodward W. Fischer[3], and Shawn E. McGlynn[2]*

[1]*Department of Earth and Planetary Sciences, Harvard University, Cambridge, MA 02138 USA;* [2]*Earth-Life Science Institute, Tokyo Institute of Technology, Meguro, Tokyo, 152–8550, Japan;* [3]*Division of Geological and Planetary Sciences, California Institute of Technology, Pasadena, CA 91125 USA;* [4]*Department of Biological Sciences, Tokyo Metropolitan University, Hachioji, Tokyo 192–0397, Japan;* [5]*Department of Earth and Planetary Sciences, Tokyo Institute of Technology, Meguro, Tokyo, 152–8551, Japan; and* [6]*Department of Subsurface Geobiological Analysis and Research, Japan Agency for Marine-Earth Science and Technology, Natsushima-cho, Yokosuka 237–0061, Japan*

(Received February 1, 2019—Accepted May 22, 2019—Published online August 14, 2019)

Hydrothermal systems, including terrestrial hot springs, contain diverse geochemical conditions that vary over short spatial scales due to progressive interactions between reducing hydrothermal fluids, the oxygenated atmosphere, and, in some cases, seawater. At Jinata Onsen on Shikinejima Island, Japan, an intertidal, anoxic, iron-rich hot spring mixes with the oxygenated atmosphere and seawater over short spatial scales, creating diverse chemical potentials and redox pairs over a distance of ~10 m. We characterized geochemical conditions along the outflow of Jinata Onsen as well as the microbial communities present in biofilms, mats, and mineral crusts along its traverse using 16S rRNA gene amplicon and genome-resolved shotgun metagenomic sequencing. Microbial communities significantly changed downstream as temperatures and dissolved iron concentrations decreased and dissolved oxygen increased. Biomass was more limited near the spring source than downstream, and primary productivity appeared to be fueled by the oxidation of ferrous iron and molecular hydrogen by members of *Zetaproteobacteria* and *Aquificae*. The microbial community downstream was dominated by oxygenic *Cyanobacteria*. *Cyanobacteria* are abundant and active even at ferrous iron concentrations of ~150 μM, which challenges the idea that iron toxicity limited cyanobacterial expansion in Precambrian oceans. Several novel lineages of Bacteria are also present at Jinata Onsen, including previously uncharacterized members of the phyla *Chloroflexi* and *Calditrichaeota*, positioning Jinata Onsen as a valuable site for the future characterization of these clades.

Key words: geomicrobiology, Proterozoic, microaerobic, astrobiology, ferruginous, thermophiles

A major theme of environmental microbiology has been the enumeration of microbial groups with the capacity to exploit the diverse chemical potentials (*i.e.* chemical disequilibria) that occur in nature (*e.g.* 7, 25, 111). Hot springs, with their varied chemical compositions, provide reservoirs of novel microbial diversity; environmental and geochemical conditions in these environments select lineages and metabolic pathways that are distinct from other Earth-surface environments (*e.g.* 3, 9, 26, 126, 127). In addition to their value as sources of microbial diversity, hot springs are valuable test beds for understanding microbial community processes driven by different suites of metabolism (*e.g.* 50). This in turn allows these systems to serve as process analogs and also to provide a window into biosphere functions during early times in Earth history, for example when the O_2 content of surface waters was low or non-existent. Most surface ecosystems today are fueled entirely by oxygenic photosynthesis by plants, algae, and *Cyanobacteria*; in contrast, hot spring microbial communities are commonly supported by lithotrophic or anoxygenic phototrophic organisms that derive energy and electrons for carbon fixation by oxidizing geologically sourced electron donors such as Fe^{2+}, sulfide, arsenite, and molecular hydrogen (*e.g.* 34, 63, 69, 105, 126). These communities may therefore provide insight into the flow of energy and mass that characterized microbial communities on the early Earth or even other planets, in which oxygenic photosynthesis may be absent or less significant and anoxygenic photosynthetic or lithotrophic metabolisms may play a larger role, resulting in lower overall rates of primary productivity (*e.g.* 12, 63, 97, 131–133).

Here, we present a geomicrobiological characterization of a novel Precambrian Earth process analog site: Jinata Onsen on Shikinejima Island, Tokyo Prefecture, Japan. While a small number of metagenome-assembled genomes have previously been recovered from Jinata (125, 127), we describe here the first overall characterization of the geochemistry and microbial community of this site. This site supports sharp gradients in geochemistry that in some ways recapitulate spatially environmental transitions that occurred temporally during Proterozoic time. The modern, sulfate-rich, well-oxygenated ocean that we see today is a relatively recent state, typical of only the last few hundred million years (*e.g.* 76). For the first half of Earth history, until ~2.3 billion years ago (Ga), the atmosphere and oceans were anoxic (52), and the oceans were

* Corresponding authors.
Lewis M. Ward: E-mail: lewis_ward@fas.harvard.edu;
Tel: +1–617–998–1750; Fax: +1–617–384–7396.
Shawn E. McGlynn: E-mail: mcglynn@elsi.jp;
Tel: +81–3–5734–3414; Fax: +81–3–5734–3416.

rich in dissolved iron but poor in sulfur (120). Following the Great Oxygenation Event ~2.3 Ga, the atmosphere and surface waters accumulated oxygen, and the oceans became more strongly redox stratified with oxygenated surface waters and anoxic deeper waters, rich in either dissolved iron or sulfide (88). At Jinata Onsen, this range of geochemical conditions is recapitulated over just a few meters, providing an ideal space-for-time analog to test hypotheses of how microbial diversity and productivity may have varied as environmental conditions changed through Earth history.

At Jinata hot spring, anoxic, iron-rich hydrothermal fluids feed a subaerial spring that flows into a small bay, and mixes with seawater over the course of a few meters. Over its course, the waters transition from low-oxygen, iron-rich conditions analogous to some aspects of early Proterozoic oceans, toward iron-poor and oxygen-rich conditions typical of modern coastal oceans. In upstream regions of the stream where oxygenic *Cyanobacteria* are at very low abundance, biomass is visibly sparse; however, downstream, biomass accumulates in the form of thick microbial mats containing abundant *Cyanobacteria*. Visible differences in accumulation and appearance of biomass across the temperature and redox gradient establish the hypothesis that microbial community composition, as well as the magnitude and metabolic drivers of primary productivity, varies along the spring flow. To begin testing this hypothesis and to provide a baseline description of the geochemistry and microbiology of this site in support of future investigation, we performed geochemical measurements, 16S rRNA gene amplicon sequencing, and genome-resolved metagenomic sequencing to recover draft genomes of diverse novel microbial lineages that inhabit Jinata Onsen.

Materials and Methods

Geological context and sedimentology of Jinata

Jinata Onsen is located at 34.318 N, 139.216 E on the island of Shikinejima, Tokyo Prefecture, Japan. Shikinejima is part of the Izu Islands, a chain of volcanic islands that formed in the last few million years along the northern edge of the Izu-Bonin-Mariana Arc (56). Shikinejima is formed of Late Paleopleistocene- to-Holocene non-alkaline felsic volcanics and Late-Miocene to Pleistocene non-alkaline pyroclastic volcanic flows, with Jinata Onsen located on a small bay on the southern side of the island (Fig. 1).

Sample collections

Five sites were sampled at Jinata Onsen: the Source Pool, Pool 1, Pool 2, Pool 3, and the Outflow (Fig. 1 and 2). During the first sampling trip in January 2016, two whole community DNA samples were collected from each site for 16S rRNA gene amplicon sequencing. During the second sampling trip, additional DNA was collected from the Source Pool and Pool 2 for shotgun metagenomic sequencing along with gas samples for qualitative analysis. Samples for quantitative gas analysis were collected in October 2017 and April 2018.

Samples were collected as mineral scrapings of loosely attached, fluffy iron oxide coatings from surfaces and clasts upstream (Source Pool and Pool 1) and as samples of microbial mats downstream (Pools 2 and 3 and Outflow) using sterile forceps and spatulas (~0.25 cm^3 of material). Immediately after sampling, cells were lysed and DNA was preserved with a Zymo Terralyzer BashingBead Matrix and Xpedition Lysis Buffer. Lysis was achieved by attaching tubes to the blade of a cordless reciprocating saw (Black & Decker, Towson, MD, USA) and operating for 1 min. Aqueous geochemistry samples consisted of water collected with sterile syringes and filtered through a 0.2-µm filter. Gas samples were collected near sites of ebullition emerging from the bottom of the Source Pool; collection was performed into serum vials by water substitution that were then sealed underwater to prevent contamination by air.

Geochemical analysis

Dissolved oxygen (DO), pH, and temperature measurements were performed *in situ* using an Extech DO700 8-in-1 Portable Dissolved Oxygen Meter (FLIR Commercial Systems, Nashua, NH, USA). In upstream regions at which water temperatures were higher than the operating temperature of the oxygen probe (50°C), DO concentrations were estimated by filling a 50-mL Falcon tube with spring water, sealing the tube to prevent gas exchange, and allowing the water to cool to acceptable temperatures before reopening the tube and immediately measuring oxygen concentrations, thereby

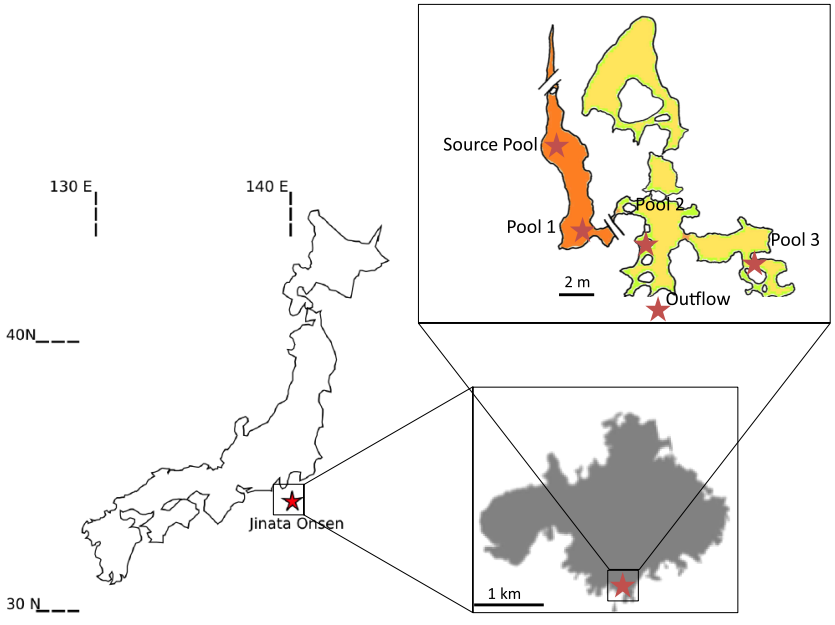

Fig. 1. Location of Jinata Onsen on Shikinejima Island, Japan, and inset overview sketch of the field site with sampling localities marked.

Fig. 2. Representative photos of Jinata. A) Panorama of the field site, with the Source Pool on the left (Pool 1 below), Pools 2 and 3 in the center, and the Outflow to the bay on the right. B) Undistorted view north up the canyon. C) Undistorted view south towards the bay, overlooking Pool 2. D) The Source Pool, coated in floc-y iron oxides and bubbling with a gas mixture containing CO_2, CH_4 and trace, potentially variable, H_2. E) Pool 2, with a mixture of red iron oxides and green from *Cyanobacteria*-rich microbial mats. F) Close up of textured microbial mats in Pool 3. G) Close up of the Outflow, at which hot spring water mixes with ocean water. Reprinted with permission from (127).

minimizing the dissolution of atmospheric O_2. Iron concentrations were measured using the ferrozine assay (110) following acidification with 40 mM sulfamic acid to inhibit iron oxidation by O_2 or oxidized nitrogen species (67). Ammonia/ammonium concentrations were measured using a TetraTest NH_3/NH_4^+ Kit (TetraPond, Blacksburg, VA, USA) following the manufacturer's instructions, but with the colorimetry of samples and NH_4Cl standards quantified with a Thermo Scientific Nanodrop 2000c spectrophotometer (Thermo Fisher Scientific, Waltham, MA, USA) at 700 nm to improve sensitivity and accuracy. Anion concentrations were measured via ion chromatography on a Shimadzu Ion Chromatograph (Shimadzu, Kyoto, Japan) equipped with a Shodex SI-90 4E anion column (Showa Denko, Tokyo, Japan).

The presence of H_2 and CH_4 in gas samples was initially qualitatively assessed by comparison to standards with a Shimadzu GC-14A gas chromatograph within 12 h of collection in order to minimize the oxidation of reduced gases. Subsequent gas samples were analyzed according to previously described methods (112). In brief, samples were analyzed using a gas chromatograph (GC-4000; GL Sciences, Tokyo, Japan) equipped with both a pulsed discharge detector (PDD) and thermal conductivity detector (TCD). The GC was equipped with a ShinCarbon ST packed column (2 m×2.2 mm ID, 50/80 mesh) connected to a HayeSepo Q packed column (2 m×2.2 mm ID, 60/80 mesh) to separate O_2, N_2, CO_2, and light hydrocarbons. Temperature was maintained at 40°C for 6 min before ramping up to 200°C at 20°C min^{-1}. This temperature was held for 6 min before ramping up to 250°C at 50°C min^{-1} before a final hold for 15 min. The values of standard errors (SE) were obtained by replicate measurements of samples. The detection limit was on the order of 1 nmol cc^{-1} for H_2 and CH_4.

Water samples for dissolved inorganic carbon (DIC) and dissolved organic carbon (DOC) concentration measurements were collected with sterile syringes and transferred after filtering through a 0.2-µm filter to pre-vacuumed 30-mL serum vials that were sealed with butyl rubber septa and aluminum crimps.

DIC and DOC concentrations in water samples were analyzed by measuring CO_2 in the headspace of the sampled vials after the reaction of samples with either phosphoric acid for DIC or potassium persulfate for DOC with a Shimadzu GC-14A gas chromatograph. Sodium bicarbonate standards and glucose standards were used to make calibration curves for quantifying DIC and DOC concentrations, respectively.

16S rRNA gene amplicon and metagenomic sequencing and analyses

The sequencing and analysis of 16S rRNA gene amplicon data followed previously described methods (126). After returning to the lab, bulk environmental DNA was extracted and purified with a Zymo Soil/Fecal DNA extraction kit. The V4–V5 region of the 16S rRNA gene was PCR amplified using the archaeal and bacterial primers 515F (GTGCCAGCMGCCGCGGTAA) and 926R (CCGY CAATTYMTTTRAGTTT) (14). DNA was quantified with a Qubit 3.0 fluorimeter (Life Technologies, Carlsbad, CA, USA) following the manufacturer's instructions after the DNA extraction and PCR steps. The successful amplification of all samples was verified by viewing on a gel after initial pre-barcoding PCR (30 cycles). Duplicate PCR reactions were pooled and reconditioned for five cycles with barcoded primers. Samples for sequencing were submitted to Laragen (Culver City, CA, USA) for analysis on an Illumina MiSeq platform. Sequence data were processed using QIIME version 1.9.1 (13). Raw sequence pairs were joined and quality-trimmed using the default parameters in QIIME. Sequences were clustered into *de novo* operational taxonomic units (OTUs) with 99% similarity using the UCLUST open reference clustering protocol (24). The most abundant sequence was selected as the representative for each *de novo* OTU (121). Taxonomic identification for each representative sequence was assigned using the Silva-132 database (90) clustered

separately at 99 and 97% similarities. Singletons and contaminants (OTUs appearing in negative control datasets) were removed. 16S rRNA gene sequences were aligned using MAFFT (60) and a phylogeny constructed using FastTree (89). Alpha diversity was estimated using the Shannon Index (96) and Inverse Simpson metric (1/D) (46, 100). Sampling depths were estimated using Good's Coverage (35). All statistics were calculated using scripts in QIIME and reported at the 99 and 97% OTU similarity levels. Multidimensional scaling (MDS) analyses and plots to evaluate similarities between different samples and environments were produced in R using the vegan and ggplot2 packages (91, 135) (Oksanen, J., F.G. Blanchet, M. Friendly, *et al.* 2016. Vegan: community ecology package. R package version 2.3-5. R Foundation, Vienna, Austria).

Following initial characterization via 16S rRNA gene sequencing, four samples were selected for shotgun metagenomic sequencing: JP1-A and JP3-A from the first sampling trip, and JP1L-1 and JP2-1 from the second sampling trip. Purified DNA was submitted to SeqMatic LLC (Fremont, CA, USA) for library preparation and 2×100-bp paired-end sequencing via Illumina HiSeq 4000 technology. Samples JP1-A and JP3-A shared a single lane with two samples from another project, while JP1L-1 and JP2-1 shared a lane with one sample from another project.

Raw sequence reads from all four samples were co-assembled with MegaHit v. 1.02 (75) and genome bins constructed based on nucleotide composition and differential coverage using MetaBAT (57), MaxBin (136), and CONCOCT (Alneberg, J., B.S. Bjarnason, I. de Bruijn, M. Schirmer, J. Quick, U.Z. Ijaz, N.J. Loman, A.F. Andersson, and C. Quince. 2013. CONCOCT: clustering contigs on coverage and composition. arXiv preprint arXiv:1312.4038.) prior to dereplication and refinement with DAS Tool (99) to produce the final bin set. Genome bins were assessed for completeness, contamination, and strain-level heterogeneity using CheckM (85), tRNA sequences found with Aragorn (71), and the presence of metabolic pathways of interest predicted with MetaPOAP (130). Coverage was extracted using bbmap (Bushnell, B. 2016. BBMap short read aligner. University of California, Berkeley, California. URL: http://sourceforge.net/projects/bbmap.) and samtools (74). Genes of interest (*e.g.* coding for ribosomal, photosynthesis, iron oxidation, and electron transport proteins) were identified from assembled metagenomic data locally with BLAST+ (10) and were screened against outlier (*e.g.* likely contaminant) contigs as identified by CheckM using tetranucleotide, GC, and coding density contents. Translated protein sequences of genes of interest were aligned with MUSCLE (23), and alignments were manually curated in Jalview (134). Phylogenetic trees were calculated using RAxML (106) on the Cipres science gateway (80). Node support for phylogenies was calculated with transfer bootstraps by BOOSTER (72). Trees were visualized with the Interactive Tree of Life viewer (73). Since the sequencing depth of each sample in the full metagenome was uneven, the relative abundance of genes of interest between metagenomic datasets was normalized to the coverage of *rpoB* genes in each raw dataset as mapped onto the co-assembly. Similar to the 16S rRNA gene, *rpoB* is a highly conserved, vertically-inherited gene that is useful for the taxonomic identification of organisms, but has the added advantage that it is only known to occur as a single copy per genome (15) and is more readily assembled in metagenomic datasets (*e.g.* 127). The presence and classification of hydrogenase genes was performed with HydDB (103). The taxonomic assignment of MAGs was made based on placement in a reference phylogeny built with concatenated ribosomal protein sequences following methods from Hug *et al.* (48), and confirmed using GTDB-Tk (86). The optimal growth temperatures of MAGs were predicted based on proteome-wide 2-mer amino acid compositions following previously described methods (Li, G., K.S. Rabe, J. Nielsen, and M.K. Engqvist. 2019. Machine learning applied to predicting microorganism growth temperatures and enzyme catalytic optima. BioRxiv. doi: https://doi.org/10.1101/522342).

Results

Site description

The source water of Jinata Onsen emerges with low DO concentrations near our limit of detection, is iron-rich, and gently bubbles gas from the spring source (Fig. 1 and 2, and Table 1). Temperatures at the source are ~63°C. Water emerges into the Source Pool, which has no visible microbial mats or biofilms (Fig. 2D). Surfaces are instead coated with a fluffy red precipitate, likely a poorly ordered or short range-ordered ferric iron oxide phase such as ferrihydrite. Flow from the source is, at least partially, tidally charged, with the highest water levels and flow rates occurring at high tide. At low tide, flow rates drop and the water level of the Source Pool may decrease by decimeters, with portions of the Source Pool potentially draining during spring low tides. Spring water collects downstream into a series of pools (Pools 1-3) (Fig. 2C, E, and F), which cool sequentially (Fig. 3 and Table S1). Pool 1 contains iron oxides, similar to the Source Pool, but also develops macroscopic microbial streamers that are coated in iron oxides and thin veil-like layers of microorganisms overlaying iron oxide sediments—structures similar to those typically made by marine iron-oxidizing *Zetaproteobacteria* (*e.g.* 33). Streamers are very fine (mm-scale) and delicate (break apart on contact with forceps) but can reach several centimeters in length. *Cyanobacteria* in Pools 2 and 3 display high levels of photosynthetic activity as revealed by high DO concentrations (~234 μM), low DIC concentrations, and the accumulation of visible O_2 bubbles on the surface and within the fabric of the mat. Downstream pools (Pools 2 and 3) mix with seawater during high tide due to wave action; however, this seawater influence does not appear to influence the Source Pool or Pool 1. Samples were collected and temperatures were measured at high tide, reflecting the lowest temperatures experienced by microbes in the pools; at low tide, hot spring input is dominant and temperatures rise (observed range at each site in Table S1). Subaqueous surfaces in Pools 2 and 3 are covered in thick microbial mats. In Pool 2, the mat is coated in a layer of fluffy iron oxide similar to that in the Source Pool, with a dense microbial mat below (Fig. 2E). Pool 3 contains only patchy iron oxides, with mostly exposed microbial mats displaying a finger-like morphology. These "fingers" were 0.5–1 cm in diameter, up to ~5 cm long and were closely packed and carpeting surfaces of Pool 3 below the high tide line, potentially related to turbulent mixing from wave action during high tide (Fig. 2F). The Outflow is the outlet of a channel connecting Pool 2 to the bay. Its hydrology is dominantly marine with small admixtures of inflowing spring water (Fig. 2G).

Table 1. Geochemistry of source water at Jinata Onsen.

T	63°C
pH	5.4
DO	4.7 μM
Fe^{2+}	261 μM
NH_3/NH_4^+	87 μM
Cl^-	654 mM
SO_4^-	17 mM
NO_3^-	<1.6 μM
NO_2^-	<2.2 μM
HPO_4^-	<1 μM

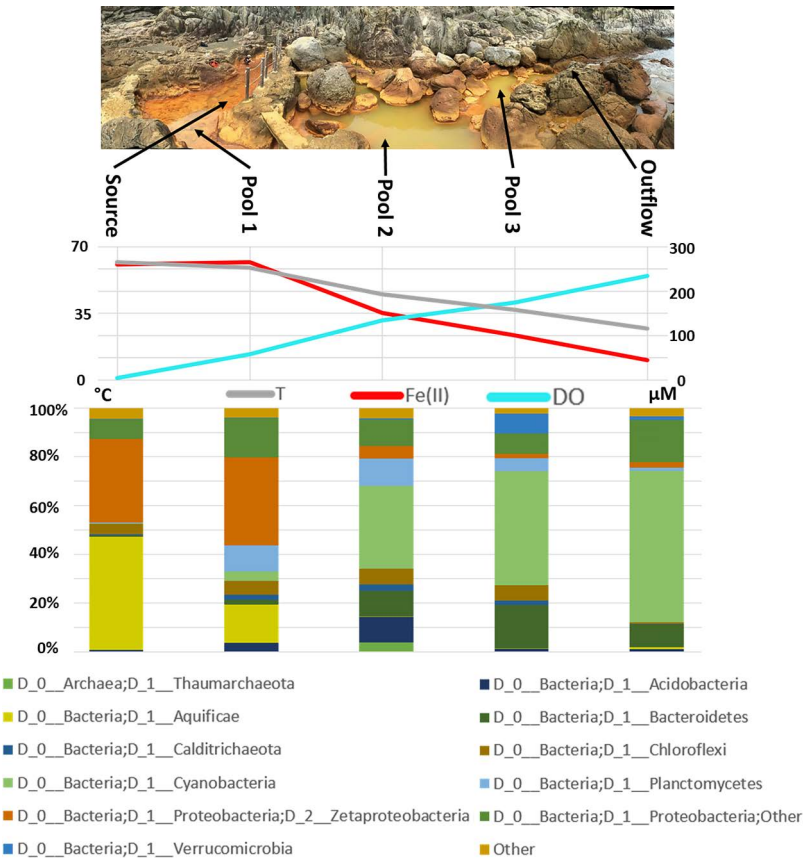

Fig. 3. Summary of geochemical and microbiological trends along the flow path of Jinata Onsen. Top: Panoramic view of Jinata Onsen, with the Source Pool at the left and the flow of spring water toward the bay at the right, with sampling locations indicated. Middle: Geochemical transect across the spring, showing temperature (°C, left axis) and dissolved Fe(II) and O_2 (µM, right axis). Bottom: Stacked bar chart of the relative community abundance of dominant microbial phyla as assessed by 16S rRNA amplicon sequencing. Sequence data were binned at the phylum level and duplicate samples at each site were averaged. Reads that could not be assigned to a phylum were discarded; all phyla that do not make up more than 2% of the community at any one site have been collapsed to "Other". Near the source, the community is predominantly made up of iron- and/or hydrogen-oxidizing organisms in the phyla *Proteobacteria* and *Aquificae*. As hot spring water flows downstream, it equilibrates with the atmosphere and eventually mixes with seawater, resulting in downstream cooling, the accumulation of oxygen, and loss of dissolved iron due to biological and abiotic processes. Oxygenic *Cyanobacteria* become progressively more abundant downstream. Putative hydrogen- and iron-oxidizing lithotrophs dominate near the source, whereas phototrophic *Cyanobacteria* dominate downstream. Additional community diversity is found in Table S4.

Jinata hot spring was visited twice for observations and community DNA sampling in 2016 (January and September), and again for observations and gas sampling in October 2017 and April 2018. These visits corresponded to a range of tidal conditions, including a spring low and high tide in September 2016. The general features of the spring were consistent across this period (including the abundance and distribution of iron minerals and microbial mats), differing primarily in apparent tidal dependence in the flow rate and water level of the spring and the extent of the seawater influence on Pool 3. These differences in flow and mixing led to variations in water temperatures of 3–10°C (Table S1). At high tide, the flow rate of the spring increases, as does seawater influx to Pool 3. During the spring low tide, the spring flow stagnated and the water level of Source Pool and Pool 1 dropped by decimeters, with some portions draining entirely. During less extreme low tides observed on other dates, the spring flow was low but nonzero and the water level of the Source Pool did not significantly drop. While marked variability was observed in the flow rate from the spring based on tides (and resulting shifts in water level and temperature), the overall geochemistry of the source water and microbial community mostly appeared to be similar between expeditions.

Geochemistry

Geochemical measurements along the flow path of Jinata Onsen revealed a major shift from hot, low-oxygen, high-iron source water to cooler, more oxygen-rich water with less dissolved iron downstream. Geochemistry measurements of Jinata source water are summarized in Table 1, while geochemical gradients along the stream outflow are shown in Fig. 3 and Table S1. Source waters were slightly enriched in chloride relative to seawater (~23.2 g L^{-1} in Jinata source water versus ~19.4 g L^{-1} in typical seawater) and depleted in sulfate (~1.6 g L^{-1} in Jinata versus ~2.7 g L^{-1} in seawater), but approached seawater concentrations downstream as mixing increased. Water emerging from the source was 63°C, very low in DO (~4.7 µM), at pH 5.4, and contained substantial concentrations of dissolved iron (~250 µM Fe^{2+}). DOC in the water of Pool 1 was high (~1.31 mM). It is unknown whether this is produced *in situ* or if the source water emerges with high DOC. DOC and DIC both decreased along the outflow

of the spring (Table S1). After emerging from the source, the spring water exchanges gases with the air due to mixing associated with water flow and gas ebullition, and DO increased to 39 μM at the surface of the Source Pool. As water flows downstream from the Source Pool, it cools slightly, exchanges gases with the atmosphere, and intermittently mixes with seawater below Pool 1.

H_2 and CH_4 were both qualitatively detected in bubbles from the Source Pool following initial sampling in September 2016. However, during subsequent analyses to quantify the gas composition in October 2017 and April 2018, the gas was found to contain CO_2, CH_4, and N_2 (Table S2). This subsequent non-detection of H_2 may be related to temporal variability in the gas composition at Jinata (*e.g.* following tidal influence; significant variability was observed in the CO_2:N_2 ratio between two sampling dates, Table S2) or may reflect oxidation of H_2 between sampling and analysis. The detection limit of H_2 for these later measurements was ~1 nmol cc^{-1} (in the gas phase of our quantitative gas analyses, or ~1 nM in the aqueous phase [2]), well above the energetic and ecological limits for hydrogenotrophic metabolisms (*e.g.* 51) leaving open the possibility of biologically significant H_2 fluxes at Jinata around the time of sampling. The oxidation of H_2 coupled to O_2 reduction is a thermodynamically favorable process even at very low substrate concentrations (*e.g.* $\Delta_rG' < -375$ kJ mol^{-1} with substrate concentrations of 0.1 nM $H_{2(aq)}$ and 0.1 μM $O_{2(aq)}$, below our limit of detection) (30). Consistent with this thermodynamic favorability, biology has been shown to make use of this metabolism in environments such as hot springs with H_2 concentrations near our detection limits (19) and in Antarctic soils where microbes rely on uptake of trace atmospheric H_2 at concentrations of ~190 ppbv (51). Therefore, the trace amounts of H_2 that may be present in the source water at Jinata may be sufficient to support lithoautotrophy near the hot spring source in organisms possessing the genetic capacity for hydrogen oxidation, as discussed below. Metagenomic data suggest that organisms with the genetic capacity for hydrogenotrophic metabolisms are abundant in upstream regions of Jinata (discussed below), and so it is also possible that low dissolved H_2 concentrations may be due to active biological consumption near the hot spring source. Improved quantification of H_2 concentrations, measurements of hydrogenase activity, and the productivity of hydrogenotrophic microbes will be necessary to determine the relative contribution of hydrogen oxidation to productivity at Jinata.

16S rRNA gene amplicon and genome-resolved metagenomic sequencing

16S rRNA gene amplicon and metagenomic sequencing of microbial communities at Jinata Onsen revealed a highly diverse community. In total, 16S rRNA gene amplicon sequencing recovered 456,737 sequences from the 10 samples at Jinata (Tables S3, 4, and 5). Reads per sample following filtering for quality and the removal of chimeras ranged between 2,076 for Pool 3 Sample B and 96,268 for Pool 1 Sample A (median 32,222, mean 35,479, and standard deviation 26,014). On average, 65% of the microbial community was recovered from Jinata samples at the 99% OTU level based on the Good's Coverage statistic of the 16S rRNA gene (ranging between 50% coverage in Outflow Sample A and 80% in Pool 1 Sample A) and 82% at the 97% OTU level (between 69% for Pool 2 Sample B and 93% for Pool 1 Sample B). MDS analysis (Fig. S1) demonstrates that samples from the same site were highly similar, and adjacent sites (*e.g.* Source Pool and Pool 1, Outflow and Pool 3) also showed a high degree of similarity. However, a substantial transition was observed in microbial community diversity between the most distant samples (*e.g.* Source Pool and Outflow).

Shotgun metagenomic sequencing of four samples from Jinata Onsen recovered 121 GB of data, forming a 1.48-Gb co-assembly consisting of 1,531,443 contigs with an N50 of 1,494 bp. Nucleotide composition and differential coverage-based binning of the co-assembly via multiple methods followed by dereplication and refinement resulted in a final set of 161 medium- or high-quality metagenome-assembled genomes (MAGs) following current standards (*i.e.* completeness >50% and contamination <10%) (6). These MAGs are from diverse phyla of Bacteria and Archaea (Fig. 4); metagenome and MAG statistics with tentative taxonomic assignments for recovered MAGs are shown in Table S6, while MAGs of particular interest due to their potential contribution to primary productivity at this site or due to substantial genetic or metabolic novelty are discussed in depth below and shown in phylogenetic trees alongside reference strains in Fig. 5, 6, and 7.

Discussion

As Jinata spring water flows from its source to the ocean, it transitions from hot, low-oxygen, high-iron water to cooler, iron-depleted, oxygen-rich water in downstream regions (Fig. 3). Following this geochemical transition is a major shift in the composition of the microbial community—from a high-temperature, putatively lithotrophic community which produces little visible biomass upstream, to a lower temperature community with well-developed, thick microbial mats downstream. This shift in community composition is summarized in Fig. 3, with complete diversity data in the Supplemental Information (including OTU counts per sample in Table S4 and relative abundance binned at the class level in Table S5). Below, we discuss the overall physiological and taxonomic trends across the spring sites as inferred from diversity and genomic analysis.

Potential for lithotrophic iron and hydrogen oxidation

The hot spring water emerging at the Source Pool at Jinata contains abundant dissolved Fe^{2+} and trace H_2 (though measurements of gas content varied, as discussed above) (Table 1). Although rates of carbon fixation were not measured, the appearance of (presumed) zetaproteobacterial veils and streamers together with molecular evidence for lithoautotrophic microbes suggest that these electron donors may fuel productivity and determine the microbial community upstream at the Source Pool and Pool 1, where microbial mats were not well developed. The low accumulation of visible biomass in upstream regions of Jinata is similar to other microbial ecosystems fueled by iron oxidation (*e.g.* Oku-Okuhachikurou Onsen [126], Fuschna Spring [43], and Jackson Creek [92]), in which lithotrophic communities appear capable of accumulating less organic carbon than communities fueled by oxygenic photosynthesis (including those in downstream regions at Jinata).

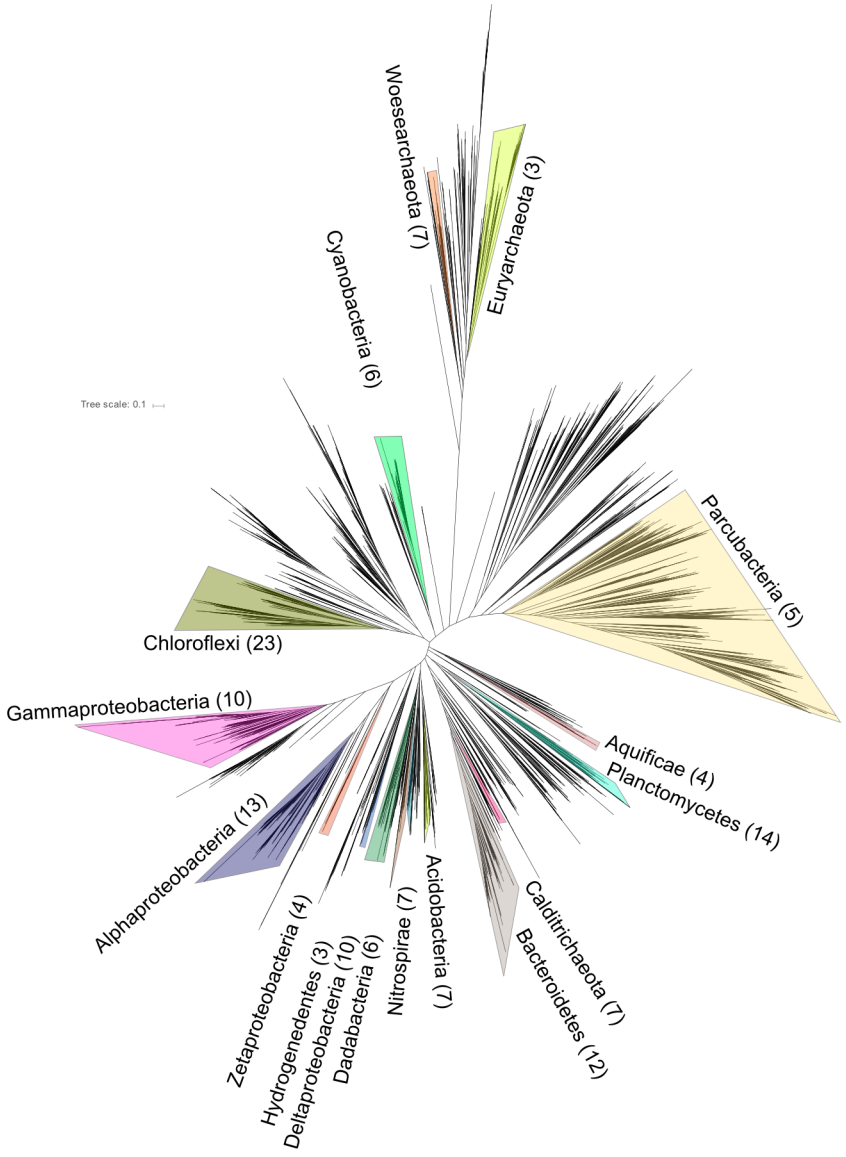

Fig. 4. Phylogeny of Bacteria and Archaea based on concatenated ribosomal proteins. Numbers in parentheses next to phylum labels refer to the number of MAGs recovered from Jinata Onsen. Labels for phyla with two or fewer MAGs recovered from Jinata were omitted for clarity. The reference alignment was modified from Hug *et al.* (48). A full list of MAGs recovered is available in Table S6.

The results of 16S rRNA gene amplicon sequencing indicate that the most abundant organisms in the Source Pool are members of the *Aquificae* family *Hydrogenothermaceae* (32% of reads in the Source Pool and 11.5% of reads in Pool 1). Members of this family are typically marine thermophilic lithotrophs capable of iron and hydrogen oxidation as well as heterotrophy (114); at Jinata, they may be utilizing Fe^{2+}, H_2, or DOC. The seventh most abundant OTU in the Source Pool samples was a novel sequence that was 89% similar to a strain of *Persephonella* observed in an alkaline hot spring in Papua New Guinea. *Persephonella* is a genus of thermophilic, microaerophilic hydrogen-oxidizing bacteria within *Hydrogenothermaceae* (36). Despite their abundance as assessed by 16S rRNA gene amplicon sequencing (Fig. 3), only four partial *Aquificae* MAGs were recovered from Jinata, of which only one (J026) was reasonably complete (~94%). Two *Aquificae* MAGs recovered Group 1 NiFe hydrogenase genes, which could support hydrogenotrophy; the absence of hydrogenases from the other MAGs may be related to their low completeness or could reflect a utilization of iron or other electron donors and not H_2 in these organisms.

The other most abundant organisms near the source are members of *Zetaproteobacteria*, a group typified by the neutrophilic, aerobic iron-oxidizing genus *Mariprofundus* common in marine systems (27). *Zetaproteobacteria* accounted for 24% of 16S rRNA gene sequences in the Source Pool and 26.5% in Pool 1. All *Zetaproteobacteria* characterized to date are obligate iron- and/or hydrogen-oxidizing lithoautotrophs (82), suggesting that these organisms play a substantial role in driving carbon fixation in the Source Pool and Pool 1.

Members of *Mariprofundaceae* have been observed to have an upper temperature limit for growth of 30°C (28), while *Zetaproteobacteria* at Jinata are found at temperatures up to 63°C. This currently represents a unique high-temperature environment for these organisms. In particular, the third most abundant OTU in the Source Pool and Pool 1 sample A is an

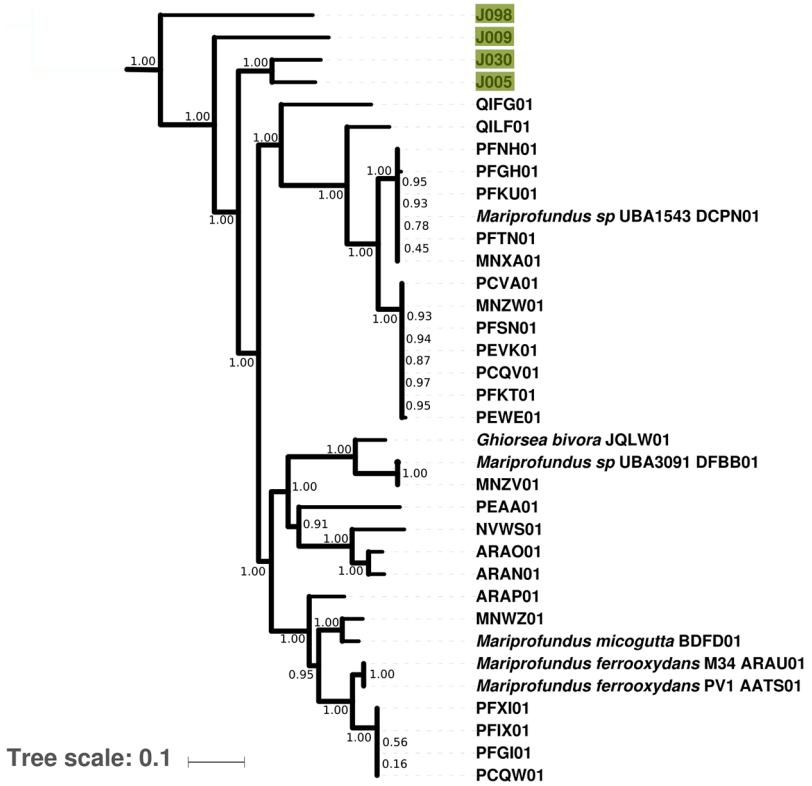

Fig. 5. Phylogeny of *Zetaproteobacteria*, rooted with *Alphaproteobacteria*, built with concatenated ribosomal protein sequences. Data from (77), (82), (101), and other draft genomes available on Genbank. Transfer bootstrap expectation (TBE) support values as calculated by BOOSTER (72) shown for internal nodes. In cases for which reference genomes have a unique strain name or identifier, this is included; otherwise Genbank WGS genome prefixes are used.

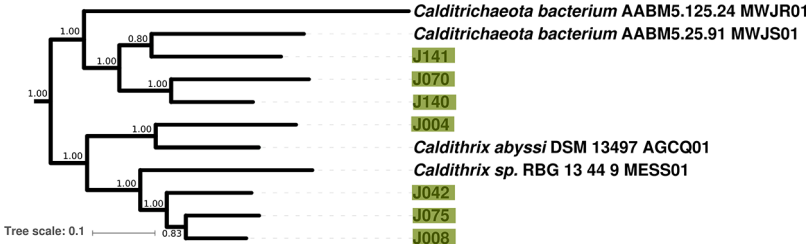

Fig. 6. Phylogeny of *Calditrichaeota*, rooted with *Bacteroidetes*, built with concatenated ribosomal protein sequences. Transfer bootstrap expectation (TBE) support values as calculated by BOOSTER (72) shown for internal nodes. Data from (68) and other draft genomes available on Genbank. In cases where reference genomes have a unique strain name or identifier, this is included; otherwise Genbank WGS genome prefixes are used.

unknown sequence that is 92% identical to a sequence from an uncultured zetaproteobacterium from a shallow hydrothermal vent in Papua New Guinea (79). This sequence likely marks a novel lineage of high-temperature iron-oxidizing *Zetaproteobacteria*.

The relative abundance of *Hydrogenothermaceae* decreases to less than 1% of sequences in areas where microbial mats are well developed downstream of Pool 1; however, *Zetaproteobacteria* continue to account for ~1–4% of reads in Pools 2 and 3 in which dissolved iron concentrations are still significant (Fig. 3). This relative abundance change may be due more to the increased abundance of other organisms rather than a decrease in the number of *Zetaproteobacteria* or their ability to make a living oxidizing iron. This hypothesis awaits confirmation by a technique such as qPCR. In contrast, the absence of *Hydrogenothermaceae* downstream may be a real signal driven by the rapid disappearance of trace H_2 as an electron donor. However, in both cases, a drop in relative abundance is likely related to the increasing total biomass (*i.e.* number of cells) downstream as *Cyanobacteria* become more productive, leading to sequences from *Hydrogenothermaceae* and *Zetaproteobacteria* being diluted out by increased numbers of *Cyanobacteria*, *Chloroflexi*, and other sequences.

Four MAGs affiliated with *Zetaproteobacteria* were recovered from Jinata with completeness estimates by CheckM ranging between ~80 and ~97% (J005, J009, J030, and J098). While these MAGs did not recover 16S rRNA genes, RpoB- and concatenated ribosomal protein-based phylogenies illustrated that members of this group at Jinata Onsen do not belong to the characterized genera *Mariprofundus* or *Ghiorsea*, but instead form separate basal lineages within *Zetaproteobacteria* (Fig. 5). Despite their phylogenetic distinctness, these MAGs largely recovered genes associated with aerobic iron oxidation as expected based on the physiology of other *Zetaproteobacteria*. These include a terminal O_2 reductase

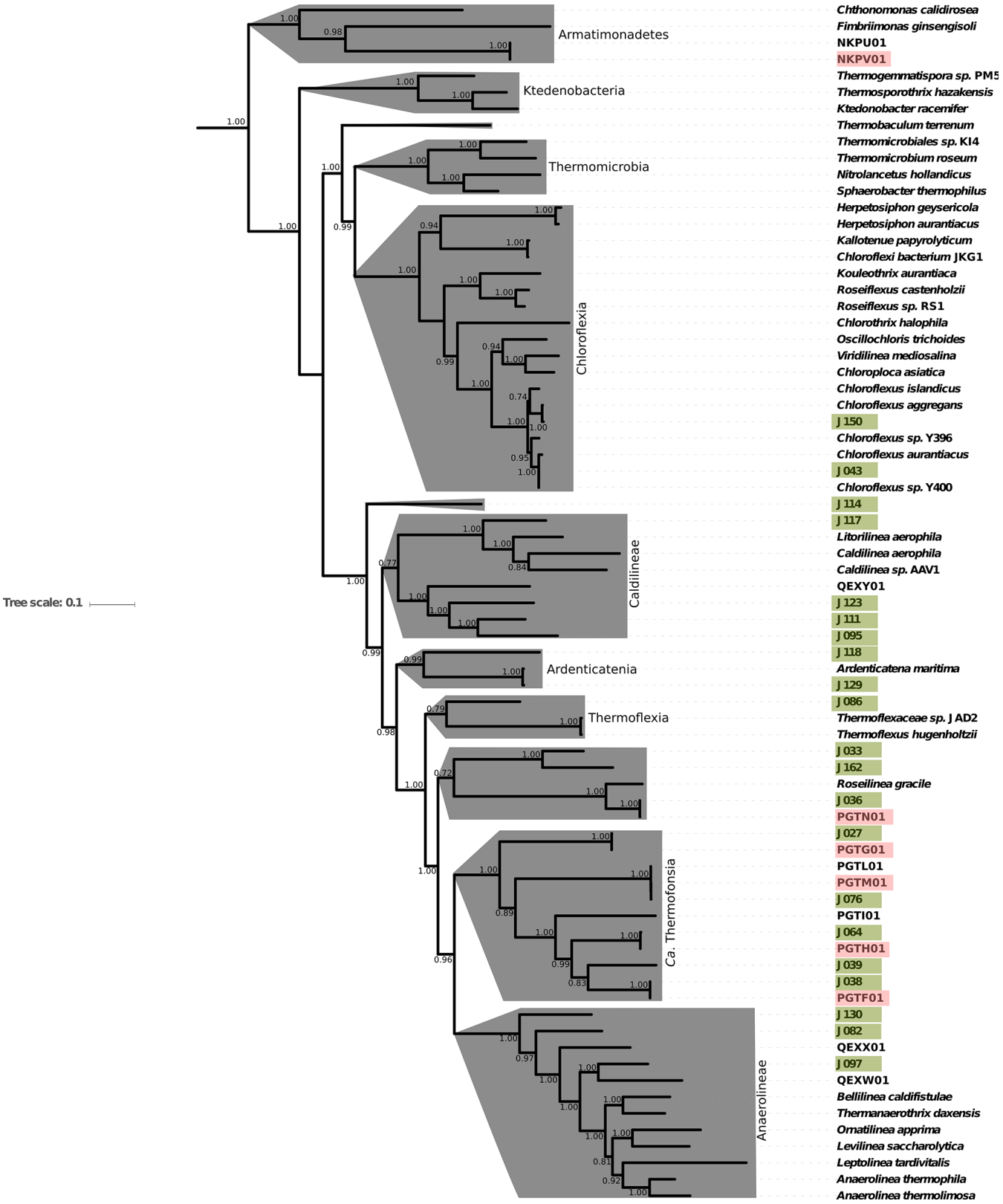

Fig. 7. Detailed phylogeny of the phylum *Chloroflexi*, with class-level clades highlighted in gray, built with concatenated ribosomal protein sequences. The large basal class *Dehalococcoidia*, which was not observed in 16S rRNA or metagenome data from Jinata, is omitted for clarity. The phylogeny contains MAGs reported here, members of the phylum *Chloroflexi* previously described (16, 20, 38, 41, 43–45, 62, 70, 83, 104, 122, 123, 127–129), and members of the closely related phylum *Armatimonadetes* as an outgroup (21, 125). MAGs described here are highlighted in green, and MAGs previously reported from Jinata Onsen are highlighted in pink. Transfer bootstrap expectation (TBE) support values as calculated by BOOSTER (72) shown for internal nodes. In cases for which reference genomes have a unique strain name or identifier, this is included; otherwise Genbank WGS genome prefixes are used.

from the C-family of heme copper oxidoreductases for respiration at low O_2 concentrations and *Cyc2* cytochrome genes implicated in ferrous iron oxidation in *Zetaproteobacteria* and other taxa (*e.g. Chlorobi*) (39, 40, 59). Hydrogenase catalytic subunit genes (neither [NiFe] nor [FeFe]) were not recovered in zetaproteobacterial MAGs even at high completeness, suggesting that these organisms are not hydrogenotrophic. Consistent with the obligately autotrophic lifestyle of previously characterized *Zetaproteobacteria*, J009 and J098 encode carbon fixation via the Calvin cycle. However, J005 and J030 did not recover genes for carbon fixation via the Calvin cycle such as the large and small subunits of rubisco, phosphoribulose kinase, or carboxysome proteins. The high completeness of these MAGs (~94–97%) makes it unlikely that these genes would all fail to be recovered (MetaPOAP False Negative estimates 10^{-5}–10^{-7}). The absence of carbon fixation pathways from these genomes together with the availability of abundant DOC in Pool 1 (~1.3 mM) suggest that these organisms may be heterotrophic, a lifestyle not previously observed for members of *Zetaproteobacteria*.

Seven MAGs were recovered from the enigmatic bacterial phylum *Calditrichaeota* (J004, J008, J042, J070, J075, J140, and J141) (Fig. 6). While few members of *Calditrichaeota* have been isolated or sequenced, the best known of these is *Caldithrix abyssi* (81); this taxon was characterized as an anaerobic thermophile capable of lithoheterotrophic H_2 oxidation coupled to denitrification and organoheterotrophic fermentation (1, 78). The *Calditrichaeota* MAGs reported here are up to 97% complete (J004) and contain members with variable putative metabolic capabilities, potentially including aerobic hydrogen- or iron-oxidizing lithoautotrophy. In the *Calditrichaeota* MAGs recovered from Jinata Onsen, aerobic respiration via A-family heme copper oxidoreductases could potentially be coupled to autotrophic hydrogen oxidation (via the Group 1d NiFe hydrogenase in J042) or iron oxidation (via the *pioA* gene in J075); however, *C. abyssi* appears incapable of aerobic respiration despite encoding an A-family heme copper oxidoreductase (68). A MAG from a member of *Calditrichaeota* has previously been recovered from Chocolate Pots hot spring in Yellowstone National Park (32); together with the data presented here this suggests that this phylum may be a common member of microbial communities in iron-rich hot springs. Unlike previously described *Calditrichaeota* which are all heterotrophic (78), most of the *Calditrichaeota* MAGs reported here possess a putative capacity for carbon fixation via the Calvin cycle. J004 is closely related to *C. abyssi*, while the other MAGs form two distinct but related clades (Fig. 6).

Oxygenic photosynthesis

Cyanobacteria are nearly absent from the Source Pool (<0.15% relative abundance), but are observed at low numbers in Pool 1 and become abundant starting in Pool 2. The most abundant *Cyanobacteria* present are predominantly members of *Nostocales*. This group includes *Leptolyngbya* and *Phormidium*, genera of filamentous non-heterocystous *Cyanobacteria* that are present in other hot springs of similar temperatures (*e.g.* 5, 94, 126). Diverse cyanobacterial MAGs were recovered, including members of the orders *Pleurocapsales* (J083), *Chroococcales* (J003 and J149), and *Oscillatoriales* (J007, J055, and J069). In Outflow samples, chloroplast sequences related to the diatom *Melosira* were abundant.

Cyanobacteria are sometimes underrepresented in 16S rRNA gene amplicon sequencing datasets as a result of a poor DNA yield or amplification biases (*e.g.* 84, 118); however, the low abundance of *Cyanobacteria* near the Source Pool was confirmed by fluorescent microscopy, in which cells displaying cyanobacterial autofluorescence were abundant in downstream samples, but not in samples from the Source Pool (Fig. S2). Thick microbial mats initially appear in Pool 2 when *Cyanobacteria* become abundant, suggesting that oxygenic photosynthesis fuels more net carbon fixation than lithotrophy in these environments.

It has been suggested that high ferrous iron concentrations are toxic to *Cyanobacteria*, and that this would have greatly reduced their productivity under ferruginous ocean conditions such as those that may have persisted through much of the Archean era (113). The abundant *Cyanobacteria* observed to be active at Jinata under high iron concentrations suggest that *Cyanobacteria* can adapt to ferruginous conditions, and therefore iron toxicity might not inhibit *Cyanobacteria* over geological timescales. Indeed, the soluble iron concentrations observed at Jinata are higher (150–250 μM) than predicted for the Archean oceans (<120 μM, 47) or observed at other iron-rich hot springs (~100–200 μM, 87, 126), making Jinata an excellent test case for determining the ability of *Cyanobacteria* to adapt to high iron concentrations. Culture-based physiological experiments may be useful to determine whether Jinata *Cyanobacteria* utilize similar strategies to other iron-tolerant strains (e.g. by those in Chocolate Pots Hot Spring, 87, or the ferric iron-tolerant *Leptolyngbya*-relative *Marsacia ferruginose*, 8) or whether Jinata strains possess unique adaptations that allow them to grow at higher iron concentrations than known for other environmental *Cyanobacteria* strains. This will in turn provide insight into whether iron tolerance is due to evolutionarily conserved strategies or whether this is a trait that has evolved convergently multiple times.

Diverse novel Chloroflexi *from Jinata Onsen*

In addition to the primary phototrophic and lithotrophic carbon fixers at Jinata, 16S rRNA gene and metagenomic data sets revealed diverse novel lineages within the phylum *Chloroflexi*. Twenty-three *Chloroflexi* MAGs were recovered, introducing substantial genetic and metabolic diversity that expands our understanding of this group. While the best known members of this phylum are Type 2 Reaction Center-containing lineages such as *Chloroflexus* and *Roseiflexus* within the class *Chloroflexia* (*e.g.* 117), phototrophy is not a synapomorphy of the phylum *Chloroflexi* or even the class *Chloroflexia* (*e.g.* 122) and most of the diversity of the phylum belongs to several other classes primarily made up of non-phototrophic lineages (127). The bulk of *Chloroflexi* diversity recovered from Jinata belongs to "subphlyum I", a broad group of predominantly non-phototrophic lineages that was originally described based on the class- or order-level lineages *Anaerolineae* and *Caldilineae* (137), but also encompasses the related groups *Ardenticatenia*, *Thermoflexia*, and *Candidatus* Thermofonsia (20, 61, 127).

16S rRNA gene analysis indicated that members of *Anaerolineae* and *Ca.* Thermofonsia (annotated by Silva and

GTDB-Tk as the order SBR1031) were fairly abundant at Jinata, with *Anaerolineae* at ~3% relative abundance in the Source Pool and Pool 1 and *Ca.* Thermofonsia at ~3.5% relative abundance in Pools 2 and 3. Three MAGs recovered from Jinata (J082, J097, and J130) are associated with the *Anaerolineae* class, as determined by RpoB and concatenated ribosomal protein phylogenies, along with seven associated with *Ca.* Thermofonsia (J027, J033, J036, J038, J039, J064, and J076). Of particular interest among these is J036, a close relative of the phototrophic *Ca.* Roseilinea gracile (66, 115, 116). J036 contains a 16S rRNA gene that is 96% similar to that of *Ca.* Roseilinea gracile, and two-way AAI estimates (93) showed 73.6% similarity between the two strains, indicating that these strains are probably best classified as distinct species within the same genus. Unlike other phototrophs in the phylum *Chloroflexi* that are capable of photoautotrophy via the 3-hydroxypropionate bicycle or the Calvin cycle (65, 98), J036 and *Ca.* Roseilinea gracile do not encode carbon fixation and are likely photoheterotrophic. Previous studies suggested that the *Roseilinea* lineage belongs to *Anaerolineae* (66) or *Thermofonsia* (127). However, our updated phylogeny presented here places J036 and *Roseilinea* in a separate lineage along with J033 and J162, diverging just outside of the *Anaerolineae*+ *Thermofonsia* clade. This suggests that these strains may instead be yet another class- or order-level lineage within the broader "subphylum I" of *Chloroflexi* (Fig. 7), an interpretation supported by analysis via GTDB-Tk that places these genomes outside of characterized clades (Table S6).

The *Chloroflexi* class *Ardenticatenia* was first described from an isolate from an iron-rich Japanese hydrothermal field (61) and has since also been recovered from sulfidic hot springs (128). Members of *Ardenticatenia* were present at up to 1.2% relative abundance in Pool 3 in 16S amplicon data. One MAG recovered from Jinata Onsen, J129, was closely related to *Ardenticatena maritima*. While *A. maritima 110S* contains a complete denitrification pathway (45), MAG J129 did not recover any denitrification genes. This may be related to the relatively low completeness of this MAG (~70%); however, MetaPOAP (131) False Negative estimates for the probability that all four steps in the canonical denitrification pathway would fail to be recovered in J129 given their presence in the source genome is less than 0.8%. This suggests that most, if not all denitrification genes are absent from the J129 genome and that the capacity for denitrification is not universal within members of *Ardenticatena*. This would be consistent with broad trends in the apparently frequent modular horizontal gene transfer of partial denitrification pathways between disparate microbial lineages to drive rapid adaption and metabolic flexibility of aerobic organisms in microoxic and anoxic environments, for reasons that are still not well established (17, 109).

Members of the *Chloroflexi* class *Caldilineae* were present at up to 0.5% abundance at Jinata in the 16S rRNA gene dataset. Members of *Caldilineae* have previously been isolated from intertidal hot springs in Iceland (55) and Japanese hot springs (95). Characterized organisms in this class are filamentous, anaerobic, or facultatively aerobic heterotrophs (37, 55, 95); therefore, these taxa may play a role in degrading biomass within low-oxygen regions of microbial mats at Jinata. Three MAGs were recovered that form a deeply branching lineage within the *Caldilineae* class (J095, J111, and J123), sister to the previously characterized genera *Caldilinea* and *Litorilinea*. Like other members of *Caldilineae*, these strains encode aerobic respiration via A-family heme copper oxidoreductases and both a *bc* complex III and alternative complex III, and are therefore likely at least facultatively aerobic. J095 also encodes carbon fixation via the Calvin cycle as well as a Group 1f NiFe hydrogenase, suggesting a potential capability for hydrogenotrophic lithoautotrophy, expanding the known metabolic diversity of this class and the *Chloroflexi* phylum as a whole.

MAG J114 branches at the base of subphylum I of *Chloroflexi*, potentially the first member of a novel class-level lineage. The divergence between *Anaerolineae* and *Caldilineae* has been estimated to have occurred on the order of 1.7 Ga (98). The phylogenetic placement of J114 suggests that it diverged from other members of subphylum I even earlier, and it may be a good target for future investigation to assess aspects of the early evolution of the phylum *Chloroflexi*. J114 encodes aerobic respiration via an A-family heme copper oxidoreductase and an alternative complex III like many other non-phototrophic *Chloroflexi* lineages (*e.g.* 122, 127) as well as a Group 1f NiFe hydrogenase and carbon fixation via the Calvin cycle, suggesting the capacity for aerobic hydrogen-oxidizing autotrophy—a lifestyle not previously described for members of *Chloroflexi*.

Conclusions

To our knowledge, this is the first overall geomicrobiological characterization of Jinata Onsen, providing baseline descriptions of geochemistry and microbial diversity in order to establish a series of testable hypotheses that can be addressed by future studies. We have also provided genome-resolved metagenomic sequencing of this site focusing on members of the microbial community predicted to be responsible for the bulk of primary productivity in this system along with other organisms belonging to novel or under-characterized lineages. However, this is just a subset of the diverse microbial populations at Jinata Onsen; many more MAGs from across the tree of life were recovered than are discussed in detail here but which may be of use to others (Fig. 4 and Table S6).

The diversity of iron-oxidizing bacteria at Jinata is different than in other Fe^{2+}-rich springs and environments. For example, in freshwater systems such as Oku-Okuhachikurou Onsen in Akita Prefecture (126) and Budo Pond in Hiroshima Prefecture, Japan (58), iron oxidation is primarily driven by the activity of chemoautotrophs such as members of *Gallionellaceae*. In contrast, at Chocolate Pots hot spring in Yellowstone National Park, USA, iron oxidation is primarily abiotic, driven by O_2 produced by *Cyanobacteria*, with only a small contribution from iron-oxidizing bacteria (32, 119). The distinct iron-oxidizing community at Jinata Onsen may be related to the salinity of the spring water, or biogeographically by access to the ocean, as *Zetaproteobacteria* are typically found in marine settings, particularly in deep ocean basins associated with hydrothermal iron sources (28). Despite the taxonomically distinct iron oxidizer communities between Jinata and Oku-Okuhachikurou Onsen, both communities support only limited visible biomass in regions dominated by iron oxidizers (126), perhaps reflecting the shared biochemical and bioenergetic

challenges of iron oxidation incurred by diverse iron-oxidizing bacteria including *Gallionellaceae* and *Zetaproteobacteria* (4, 28, 126). Future work focused on isolation and physiological characterization of these microbes, quantification of rates and determination of microbial drivers of carbon fixation and aerobic and anaerobic heterotrophy, and carbon isotope profiling of organic and inorganic species along the flow path of the hot spring will be necessary to fully characterize the activity of microbes at Jinata and to fully compare this system to other areas with high dissolved ferrous iron concentrations (*e.g.* Oku-Okuhachikurou Onsen [126], Fuschna Spring [42], Jackson Creek [92], and Chocolate Pots Hot Spring [32, 119]).

Future work aimed at a more complete understanding of the geochemistry of Jinata and its impact on microbial communities will be valuable. For example, a quantitative determination of budgets and variability of gas chemistry and DOC will be beneficial. DOC may stimulate heterotrophic activity by the microbial community at Jinata, coupled to aerobic or anaerobic respiration (such as dissimilatory iron reduction, as observed in other iron-rich hot springs, *e.g.* 31), resulting in the drawdown of DOC downstream. Since the source of this DOC is unclear, future work will be necessary to determine whether DOC is present in the source water or if it is produced *in situ* by the microbial community in the Source Pool and Pool 1. Future work is also needed to evaluate the potential for dissimilatory iron reduction and other anaerobic metabolisms including sulfate reduction and methanogenesis.

Throughout Earth history, the metabolic opportunities available to life, and the resulting organisms and metabolisms responsible for driving primary productivity, have been shaped by the geochemical conditions of the atmosphere and oceans. The modern, sulfate-rich, well-oxygenated oceans we see today reflect a relatively recent state—one typical of only the last few hundred million years (*e.g.* 76). For the first half of Earth history, until ~2.3 Ga, the atmosphere and oceans were anoxic (52), and seawater was rich in dissolved iron but poor in sulfur (120). At this time, productivity was low and fueled by metabolisms such as methanogenesis and anoxygenic photosynthesis (12, 64, 131). Following the expansion of oxygenic photosynthesis by *Cyanobacteria* and higher primary productivity around the Great Oxygenation Event ~2.3 Ga (18, 29, 124, 133), the atmosphere and surface ocean accumulated some oxygen, and the ocean transitioned into a state with oxygenated surface waters but often anoxic deeper waters, rich in either dissolved iron or sulfide (11, 53, 54, 88). At Jinata Onsen, this range of geochemical conditions is recapitulated over just a few meters, providing a useful test case for probing the shifts in microbial productivity over the course of Earth history. In particular, the concomitant increase in visible biomass at Jinata as the community shifts from lithotrophy toward water-oxidizing phototrophy (*i.e.* oxygenic photosynthesis) is consistent with estimates for greatly increased primary production following the evolution and expansion of *Cyanobacteria* around the GOE (18, 97, 102, 124, 131, 133).

The dynamic abundances of redox-active compounds including oxygen, iron, and hydrogen at Jinata may not only be analogous to conditions on the early Earth, but may have relevance for potentially habitable environments on Mars as well. Early Mars is thought to have supported environments with metabolic opportunities provided by the redox gradient between the oxidizing atmosphere and abundant electron donors such as ferrous iron and molecular hydrogen sourced from water/rock interactions (*e.g.* 49), and production of these substrates may continue today (22, 107), potentially supporting past or present life in the Martian subsurface (108). Understanding the potential productivity of microbial communities fueled by lithotrophic metabolisms is critical for setting expectations for the presence and size of potential biospheres on other worlds and early in Earth history (*e.g.* 131–133). Uncovering the range of microbial metabolisms present under the environmental conditions at Jinata, and their relative contributions to primary productivity, may therefore find application to predicting environments on Mars most able to support productive microbial communities.

Data availability

Raw 16S rRNA gene amplicon data, raw metagenomic sequence data, and MAGs have been uploaded and made publicly available on NCBI under Project Number PRJNA392119 (genome accession numbers are found in Table S6).

Acknowledgements

LMW acknowledges support from NASA NESSF (#NNX16AP39H), NSF (#OISE 1639454), NSF GROW (#DGE 1144469), the Lewis and Clark Fund for Exploration and Field Research in Astrobiology, the ELSI Origins Network, and an Agouron Institute postdoctoral fellowship. WWF acknowledges the support of NASA Exobiology award #NNX16AJ57G and the Simons Foundation Collaboration on the Origins of Life. MN and YU acknowledge the support of the Japan Society for the Promotion of Science (JP17K14412, JP17H06105)

References

1. Alauzet, C., and E. Jumas-Bilak. 2014. The phylum Deferribacteres and the genus Caldithrix, p. 595–611. *In* E. Rosenberg, E.F. Delong, S. Lory, E. Stackebrandt, and F. Thompson (ed.), The Prokaryotes. Springer, Berlin, Heidelberg.
2. Amend, J.P., and E.L. Shock. 2001. Energetics of overall metabolic reactions of thermophilic and hyperthermophilic Archaea and Bacteria. FEMS Microbiol. Rev. 25:175–243.
3. Beam, J.P., Z.J. Jay, M.C. Schmid, D.B. Rusch, M.F. Romine, R. de M Jennings, M.A. Kozubal, S.G. Tringe, M. Wagner, and W.P. Inskeep. 2016. Ecophysiology of an uncultivated lineage of Aigarchaeota from an oxic, hot spring filamentous 'streamer' community. ISME J. 10:210.
4. Bird, L.J., V. Bonnefoy, and D.K. Newman. 2011. Bioenergetic challenges of microbial iron metabolisms. Trends Microbiol. 19:330–340.
5. Bosak, T., B. Liang, T.D. Wu, S.P. Templer, A. Evans, H. Vali, J.L. Guerquin-Kern, V. Klepac-Ceraj, M.S. Sim, and J. Mui. 2012. Cyanobacterial diversity and activity in modern conical microbialites. Geobiology 10:384–401.
6. Bowers, R.M., N.C. Kyrpides, R. Stepanauskas, *et al.* 2017. Minimum information about a single amplified genome (MISAG) and a metagenome-assembled genome (MIMAG) of bacteria and archaea. Nat. Biotechnol. 35:725.
7. Broda, E. 1977. Two kinds of lithotrophs missing in nature. Z. Allg. Mikrobiol. 17:491–493.
8. Brown, I.I., D.A. Bryant, D. Casamatta, *et al.* 2010. Polyphasic characterization of a thermotolerant siderophilic filamentous cyanobacterium that produces intracellular iron deposits. Appl. Environ. Microbiol. 76:6664–6672.
9. Bryant, D.A., A.M.G. Costas, J.A. Maresca, *et al.* 2007. Candidatus Chloracidobacterium thermophilum: an aerobic phototrophic acidobacterium. Science 317:523–526.

10. Camacho, C., G. Coulouris, V. Avagyan, N. Ma, J. Papadopoulos, K. Bealer, and T.L. Madden. 2009. BLAST+: architecture and applications. BMC Bioinf. 10:421.
11. Canfield, D.E. 1998. A new model for Proterozoic ocean chemistry. Nature 396:450.
12. Canfield, D.E., M.T. Rosing, and C. Bjerrum. 2006. Early anaerobic metabolisms. Philos. Trans. R. Soc. Lond., B, Biol. Sci. 361:1819–1836.
13. Caporaso, J.G., J. Kuczynski, J. Stombaugh, *et al.* 2010. QIIME allows analysis of high-throughput community sequencing data. Nat. Methods 7:335.
14. Caporaso, J.G., C.L. Lauber, W.A. Walters, *et al.* 2012. Ultra-high-throughput microbial community analysis on the Illumina HiSeq and MiSeq platforms. ISME J. 6:1621.
15. Case, R.J., Y. Boucher, I Dahllöf, C. Holmström, W.F. Doolittle, and S. Kjelleberg. 2007. Use of 16S rRNA and rpoB genes as molecular markers for microbial ecology studies. Appl. Environ. Microbiol. 73:278–288.
16. Chang, Y.J., M. Land, L. Hauser, *et al.* 2011. Non-contiguous finished genome sequence and contextual data of the filamentous soil bacterium Ktedonobacter racemifer type strain (SOSP1-21 T). Stand. Genomic Sci. 5:97.
17. Chen, J., and M. Strous. 2013. Denitrification and aerobic respiration, hybrid electron transport chains and co-evolution. Biochim. Biophys. Acta 1827:136–144.
18. Crockford, P.W., J.A. Hayles, H. Bao, N.J. Planavsky, A. Bekker, P.W. Fralick, G.P. Halverson, T.H. Bui, Y. Peng, and B.A. Wing. 2018. Triple oxygen isotope evidence for limited mid-Proterozoic primary productivity. Nature 559:613.
19. D'Imperio, S., C.R. Lehr, H. Oduro, G. Druschel, M. Kühl, and T.R. McDermott. 2008. Relative importance of H2 and H2S as energy sources for primary production in geothermal springs. Appl. Environ. Microbiol. 74:5802–5808.
20. Dodsworth, J.A., J. Gevorkian, F. Despujos, J.K. Cole, S.K. Murugapiran, H. Ming, W.J. Li, G. Zhang, A. Dohnalkova, and B.P. Hedlund. 2014. Thermoflexus hugenholtzii gen. nov., sp. nov., a thermophilic, microaerophilic, filamentous bacterium representing a novel class in the Chloroflexi, Thermoflexia classis nov., and description of Thermoflexaceae fam. nov. and Thermoflexales ord. nov. Int. J. Syst. Evol. Microbiol. 64:2119–2127.
21. Dunfield, P.F., I. Tamas, K.C. Lee, X.C. Morgan, I.R. McDonald, and M.B. Stott. 2012. Electing a candidate: a speculative history of the bacterial phylum OP10. Environ. Microbiol. 14:3069–3080.
22. Dzaugis, M., A.J. Spivack, and S. D'Hondt. 2018. Radiolytic H2 production in martian environments. Astrobiology 18:1137–1146.
23. Edgar, R.C. 2004. MUSCLE: multiple sequence alignment with high accuracy and high throughput. Nucleic Acids Res. 32:1792–1797.
24. Edgar, R.C. 2010. Search and clustering orders of magnitude faster than BLAST. Bioinformatics 26:2460–2461.
25. Ehrenreich, A., and F. Widdel. 1994. Anaerobic oxidation of ferrous iron by purple bacteria, a new type of phototrophic metabolism. Appl. Environ. Microbiol. 60:4517–4526.
26. Eloe-Fadrosh, E.A., D. Paez-Espino, J. Jarett, *et al.*, 2016. Global metagenomic survey reveals a new bacterial candidate phylum in geothermal springs. Nat. Commun. 7:10476.
27. Emerson, D., J.A. Rentz, T.G. Lilburn, R.E. Davis, H. Aldrich, C. Chan, and C.L. Moyer. 2007. A novel lineage of proteobacteria involved in formation of marine Fe-oxidizing microbial mat communities. PLoS One 2:e667.
28. Emerson, D., E.J. Fleming, and J.M. McBeth. 2010. Iron-oxidizing bacteria: an environmental and genomic perspective. Annu. Rev. Microbiol. 64:561–583.
29. Fischer, W.W., J. Hemp, and J.E. Johnson. 2016. Evolution of oxygenic photosynthesis. Annu. Rev. Earth Planet. Sci. 44:647–683.
30. Flamholz, A., E. Noor, A. Bar-Even, and R. Milo. 2011. eQuilibrator—the biochemical thermodynamics calculator. Nucleic Acids Res. 40:D770–D775.
31. Fortney, N.W., S. He, B.J. Converse, B.L. Beard, C.M. Johnson, E.S. Boyd, and E.E. Roden. 2016. Microbial Fe (III) oxide reduction potential in Chocolate Pots hot spring, Yellowstone National Park. Geobiology 14:255–275.
32. Fortney, N.W., S. He, B.J. Converse, E.S. Boyd, and E.E. Roden. 2018. Investigating the composition and metabolic potential of microbial communities in Chocolate Pots hot springs. Front. Microbiol. 9.
33. Fullerton, H., K.W. Hager, S.M. McAllister, and C.L. Moyer. 2017. Hidden diversity revealed by genome-resolved metagenomics of iron-oxidizing microbial mats from Lō'ihi Seamount, Hawai'i. ISME J. 11:1900.
34. Giovannoni, S.J., N.P. Revsbech, D.M. Ward, and R.W. Castenholz. 1987. Obligately phototrophic Chloroflexus: primary production in anaerobic hot spring microbial mats. Arch. Microbiol. 147:80–87.
35. Good, I.J. 1953. The population frequencies of species and the estimation of population parameters. Biometrika 40:237–264.
36. Götz, D., A. Banta, T.J. Beveridge, A.I. Rushdi, B.R.T. Simoneit, and A.L. Reysenbach. 2002. Persephonella marina gen. nov., sp. nov. and Persephonella guaymasensis sp. nov., two novel, thermophilic, hydrogen-oxidizing microaerophiles from deep-sea hydrothermal vents. Int. J. Syst. Evol. Microbiol. 52:1349–1359.
37. Grégoire, P., M. Bohli, J.L. Cayol, *et al.* 2011. Caldilinea tarbellica sp. nov., a filamentous, thermophilic, anaerobic bacterium isolated from a deep hot aquifer in the Aquitaine Basin. Int. J. Syst. Evol. Microbiol. 61:1436–1441.
38. Grouzdev, D.S., M.S. Rysina, I.A. Bryantseva, V.M. Gorlenko, and V.A. Gaisin. 2018. Draft genome sequences of 'Candidatus Chloroploca asiatica' and 'Candidatus Viridilinea mediisalina', candidate representatives of the Chloroflexales order: phylogenetic and taxonomic implications. Stand. Genomic Sci. 13:24.
39. Han, H., J. Hemp, L.A. Pace, H. Ouyang, K. Ganesan, J.H. Roh, F. Daldal, S.R. Blanke, and R.B. Gennis. 2011. Adaptation of aerobic respiration to low O2 environments. Proc. Natl. Acad. Sci. U.S.A. 108:14109–14114.
40. He, S., R.A. Barco, D. Emerson, and E.E. Roden. 2017. Comparative genomic analysis of neutrophilic iron (II) oxidizer genomes for candidate genes in extracellular electron transfer. Front. Microbiol. 8:1584.
41. Hedlund, B.P., S.K. Murugapiran, M. Huntemann, *et al.* 2015. High-quality draft genome sequence of Kallotenue papyrolyticum JKG1T reveals broad heterotrophic capacity focused on carbohydrate and amino acid metabolism. Genome Announc. 3:e01410-15.
42. Hegler, F., T. Lösekann-Behrens, K. Hanselmann, S. Behrens, and A. Kappler. 2012. Influence of seasonal and geochemical changes on iron geomicrobiology of an iron-carbonate mineral water spring. Appl. Environ. Microbiol. 78:7185–7196.
43. Hemp, J., L.M. Ward, L.A. Pace, and W.W. Fischer. 2015. Draft genome sequence of Levilinea saccharolytica KIBI-1, a member of the Chloroflexi class Anaerolineae. Genome Announc. 3:e01357-15.
44. Hemp, J., L.M. Ward, L.A. Pace, and W.W. Fischer. 2015. Draft genome sequence of Ornatilinea apprima P3M-1, an anaerobic member of the Chloroflexi class Anaerolineae. Genome Announc. 3:e01353-15.
45. Hemp, J., L.M. Ward, L.A. Pace, and W.W. Fischer. 2015. Draft genome sequence of Ardenticatena maritima 110S, a thermophilic nitrate-and iron-reducing member of the Chloroflexi class Ardenticatenia. Genome Announc. 3:e01347-15.
46. Hill, M.O. 1973. Diversity and evenness: a unifying notation and its consequences. Ecology 54:427–432.
47. Holland, H.D. 1984. The Chemical Evolution of the Atmosphere and Oceans. Princeton University Press, Princeton, New Jersey.
48. Hug, L.A., B.J. Baker, K. Anantharaman, *et al.* 2016. A new view of the tree of life. Nat. Microbiol. 1:16048.
49. Hurowitz, J.A., W.W. Fischer, N.J. Tosca, and R.E. Milliken. 2010. Origin of acidic surface waters and the evolution of atmospheric chemistry on early Mars. Nat. Geosci. 3:323.
50. Inskeep, W.P., G.G. Ackerman, W.P. Taylor, M. Kozubal, S. Korf, and R.E. Macur. 2005. On the energetics of chemolithotrophy in nonequilibrium systems: case studies of geothermal springs in Yellowstone National Park. Geobiology 3:297–317.
51. Ji, M., C. Greening, I. Vanwonterghem, *et al.* 2017. Atmospheric trace gases support primary production in Antarctic desert surface soil. Nature 552:400.
52. Johnson, J.E., A. Gerpheide, M.P. Lamb, and W.W. Fischer. 2014. O2 constraints from Paleoproterozoic detrital pyrite and uraninite. Geol. Soc. Am. Bull. 126:813–830.
53. Johnston, D.T., F. Wolfe-Simon, A. Pearson, and A.H. Knoll. 2009. Anoxygenic photosynthesis modulated Proterozoic oxygen and sustained Earth's middle age. Proc. Natl. Acad. Sci. U.S.A. 106:16925–16929.
54. Johnston, D.T., S.W. Poulton, C. Dehler, S. Porter, J. Husson, D.E. Canfield, and A.H. Knoll. 2010. An emerging picture of Neoproterozoic ocean chemistry: Insights from the Chuar Group, Grand Canyon, USA. Earth Planet. Sci. Lett. 290:64–73.

55. Kale, V., S.H. Björnsdóttir, Ó.H. Friðjónsson, S.K. Pétursdóttir, S. Ómarsdóttir, and G.Ó. Hreggviðsson. 2013. Litorilinea aerophila gen. nov., sp. nov., an aerobic member of the class Caldilineae, phylum Chloroflexi, isolated from an intertidal hot spring. Int. J. Syst. Evol. Microbiol. 63:1149–1154.
56. Kaneoka, I., N. Isshiki, and S. Zashu. 1970. K-Ar ages of the Izu-Bonin islands. Geochem. J. 4:53–60.
57. Kang, D.D., J. Froula, R. Egan, and Z. Wang. 2015. MetaBAT, an efficient tool for accurately reconstructing single genomes from complex microbial communities. PeerJ. 3:e1165.
58. Kato, S., S. Kikuchi, T. Kashiwabara, Y. Takahashi, K. Suzuki, T. Itoh, M. Ohkuma, and A. Yamagishi. 2012. Prokaryotic abundance and community composition in a freshwater iron-rich microbial mat at circumneutral pH. Geomicrobiol. J. 29:896–905.
59. Kato, S., M. Ohkuma, D.H. Powell, S.T. Krepski, K. Oshima, M. Hattori, N. Shapiro, T. Woyke, and C.S. Chan. 2015. Comparative genomic insights into ecophysiology of neutrophilic, microaerophilic iron oxidizing bacteria. Front. Microbiol. 6:1265.
60. Katoh, K., K. Misawa, K.I. Kuma, and T. Miyata. 2002. MAFFT: a novel method for rapid multiple sequence alignment based on fast Fourier transform. Nucleic Acids Res. 30:3059–3066.
61. Kawaichi, S., N. Ito, R. Kamikawa, T. Sugawara, T. Yoshida, and Y. Sako. 2013. Ardenticatena maritima gen. nov., sp. nov., a ferric iron- and nitrate-reducing bacterium of the phylum 'Chloroflexi' isolated from an iron-rich coastal hydrothermal field, and description of Ardenticatenia classis nov. Int. J. Syst. Evol. Microbiol. 63:2992–3002.
62. Kawaichi, S., T. Yoshida, Y. Sako, and R. Nakamura. 2015. Draft genome sequence of a heterotrophic facultative anaerobic thermophilic bacterium, Ardenticatena maritima strain 110ST. Genome Announc. 3:e01145-15.
63. Kawasumi, T., Y. Igarashi, T. Kodama, and Y. Minoda. 1980. Isolation of strictly thermophilic and obligately autotrophic hydrogen bacteria. Agric. Biol. Chem. 44:1985–1986.
64. Kharecha, P., J. Kasting, and J. Siefert. 2005. A coupled atmosphere–ecosystem model of the early Archean Earth. Geobiology 3:53–76.
65. Klatt, C.G., D.A. Bryant, and D.M. Ward. 2007. Comparative genomics provides evidence for the 3-hydroxypropionate autotrophic pathway in filamentous anoxygenic phototrophic bacteria and in hot spring microbial mats. Environ. Microbiol. 9:2067–2078.
66. Klatt, C.G., J.M. Wood, D.B. Rusch, *et al.* 2011. Community ecology of hot spring cyanobacterial mats: predominant populations and their functional potential. ISME J. 5:1262.
67. Klueglein, N., and A. Kappler. 2013. Abiotic oxidation of Fe (II) by reactive nitrogen species in cultures of the nitrate-reducing Fe (II) oxidizer Acidovorax sp. BoFeN1–questioning the existence of enzymatic Fe (II) oxidation. Geobiology 11:180–190.
68. Kublanov, I.V., O.M. Sigalova, S.N. Gavrilov, *et al.* 2017. Genomic analysis of Caldithrix abyssi, the thermophilic anaerobic bacterium of the novel bacterial phylum Calditrichaeota. Front. Microbiol. 8:195.
69. Kulp, T.R., S.E. Hoeft, M. Asao, M.T. Madigan, J.T. Hollibaugh, J.C. Fisher, J.F. Stolz, C.W. Culbertson, L.G. Miller, and R.S. Oremland. 2008. Arsenic (III) fuels anoxygenic photosynthesis in hot spring biofilms from Mono Lake, California. Science 321:967–970.
70. Kuznetsov, B.B., R.N. Ivanovsky, O.I. Keppen, *et al.* 2011. Draft genome sequence of the anoxygenic filamentous phototrophic bacterium Oscillochloris trichoides subsp. DG-6. J. Bacteriol. 193:321–322.
71. Laslett, D., and B. Canback. 2004. ARAGORN, a program to detect tRNA genes and tmRNA genes in nucleotide sequences. Nucleic Acids Res. 32:11–16.
72. Lemoine, F., J.B.D. Entfellner, E. Wilkinson, D. Correia, M.D. Felipe, T. Oliveira, and O. Gascuel. 2018. Renewing Felsenstein's phylogenetic bootstrap in the era of big data. Nature 556:452.
73. Letunic, I., and P. Bork. 2016. Interactive tree of life (iTOL) v3: an online tool for the display and annotation of phylogenetic and other trees. Nucleic Acids Res. 44:W242–W245.
74. Li, H., B. Handsaker, A. Wysoker, T. Fennell, J. Ruan, N. Homer, G. Marth, G. Abecasis, and R. Durbin. 2009. The sequence alignment/map format and SAMtools. Bioinformatics 25:2078–2079.
75. Li, D., C.M. Liu, R. Luo, K. Sadakane, and T.W. Lam. 2015. MEGAHIT: an ultra-fast single-node solution for large and complex metagenomics assembly via succinct de Bruijn graph. Bioinformatics 31:1674–1676.
76. Lyons, T.W., C.T. Reinhard, and N.J. Planavsky. 2014. The rise of oxygen in Earth's early ocean and atmosphere. Nature 506:307.
77. Makita, H., E. Tanaka, S. Mitsunobu, M. Miyazaki, T. Nunoura, K. Uematsu, Y. Takaki, S. Nishi, S. Shimamura, and K. Takai. 2017. Mariprofundus micogutta sp. nov., a novel iron-oxidizing zetaproteobacterium isolated from a deep-sea hydrothermal field at the Bayonnaise knoll of the Izu-Ogasawara arc, and a description of Mariprofundales ord. nov. and Zetaproteobacteria classis nov. Arch. Microbiol. 199:335–346.
78. Marshall, I.P., P. Starnawski, C. Cupit, E. Fernández Cáceres, T.J. Ettema, A. Schramm, and K.U. Kjeldsen. 2017. The novel bacterial phylum Calditrichaeota is diverse, widespread and abundant in marine sediments and has the capacity to degrade detrital proteins. Environ. Microbiol. Rep. 9:397–403.
79. Meyer-Dombard, D., J.P. Amend, and M.R. Osburn. 2013. Microbial diversity and potential for arsenic and iron biogeochemical cycling at an arsenic rich, shallow-sea hydrothermal vent (Tutum Bay, Papua New Guinea). Chem. Geol. 348:37–47.
80. Miller, M.A., W. Pfeiffer, and T. Schwartz. 2010. Creating the CIPRES Science Gateway for inference of large phylogenetic trees, p. 1–8. *In* 2010 Gateway Computing Environments Workshop. (GCE), IEEE, Piscataway.
81. Miroshnichenko, M.L., N.A. Kostrikina, N.A. Chernyh, N.V. Pimenov, T.P. Tourova, A.N. Antipov, S. Spring, E. Stackebrandt, and E.A. Bonch-Osmolovskaya. 2003. Caldithrix abyssi gen. nov., sp. nov., a nitrate-reducing, thermophilic, anaerobic bacterium isolated from a Mid-Atlantic Ridge hydrothermal vent, represents a novel bacterial lineage. Int. J. Syst. Evol. Microbiol. 53:323–329.
82. Mori, J.F., J.J. Scott, K.W. Hager, C.L. Moyer, K. Küsel, and D. Emerson. 2017. Physiological and ecological implications of an iron-or hydrogen-oxidizing member of the Zetaproteobacteria, Ghiorsea bivora, gen. nov., sp. nov. ISME J. 11:2624.
83. Pace, L.A., J. Hemp, L.M. Ward, and W.W. Fischer. 2015. Draft genome of Thermanaerothrix daxensis GNS-1, a thermophilic facultative anaerobe from the Chloroflexi class Anaerolineae. Genome Announc. 3:e01354-15.
84. Parada, A.E., D.M. Needham, and J.A. Fuhrman. 2016. Every base matters: assessing small subunit rRNA primers for marine microbiomes with mock communities, time series and global field samples. Environ. Microbiol. 18:1403–1414.
85. Parks, D.H., M. Imelfort, C.T. Skennerton, P. Hugenholtz, and G.W. Tyson. 2015. CheckM: assessing the quality of microbial genomes recovered from isolates, single cells, and metagenomes. Genome Res. 25:1043–1055.
86. Parks, D.H., M. Chuvochina, D.W. Waite, C. Rinke, A. Skarshewski, P.A. Chaumeil, and P. Hugenholtz. 2018. A standardized bacterial taxonomy based on genome phylogeny substantially revises the tree of life. Nat. Biotechnol. 36:996–1004.
87. Pierson, B.K., M.N. Parenteau, and B.M. Griffin. 1999. Phototrophs in high-iron-concentration microbial mats: physiological ecology of phototrophs in an iron-depositing hot spring. Appl. Environ. Microbiol. 65:5474–5483.
88. Poulton, S.W., P.W. Fralick, and D.E. Canfield. 2010. Spatial variability in oceanic redox structure 1.8 billion years ago. Nat. Geosci. 3:486.
89. Price, M.N., P.S. Dehal, and A.P. Arkin. 2010. FastTree 2–approximately maximum-likelihood trees for large alignments. PLoS One 5:e9490.
90. Quast, C., E. Pruesse, P. Yilmaz, J. Gerken, T. Schweer, P. Yarza, J. Peplies, and F.O. Glöckner. 2012. The SILVA ribosomal RNA gene database project: improved data processing and web-based tools. Nucleic Acids Res. 41:D590–D596.
91. R Core Team. 2014. R: A Language and Environment for Statistical Computing. R Foundation for Statistical Computing, Vienna, Austria.
92. Roden, E., J.M. McBeth, M. Blothe, E.M. Percak-Dennett, E.J. Fleming, R.R. Holyoke, G.W. Luther III, and D. Emerson. 2012. The microbial ferrous wheel in a neutral pH groundwater seep. Front. Microbiol. 3:172.
93. Rodriguez-R, L.M., and K.T. Konstantinidis. 2014. Bypassing cultivation to identify bacterial species. Microbe 9:111–118.
94. Roeselers, G., T.B. Norris, R.W. Castenholz, S. Rysgaard, R.N. Glud, M. Kühl, and G. Muyzer. 2007. Diversity of phototrophic bacteria in microbial mats from Arctic hot springs (Greenland). Environ. Microbiol. 9:26–38.
95. Sekiguchi, Y., T. Yamada, S. Hanada, A. Ohashi, H. Harada, and Y. Kamagata. 2003. Anaerolinea thermophila gen. nov., sp. nov. and Caldilinea aerophila gen. nov., sp. nov., novel filamentous thermophiles that represent a previously uncultured lineage of the domain Bacteria at the subphylum level. Int. J. Syst. Evol. Microbiol. 53:1843–1851.

96. Shannon, C. 1948. A mathematical theory of communication, p. 379–423, 623–656. *In* The Bell System Technical Journal, vol. 27. University of Illinois Press, Champaign.
97. Shih, P.M., J. Hemp, L.M. Ward, N.J. Matzke, and W.W. Fischer. 2017. Crown group Oxyphotobacteria postdate the rise of oxygen. Geobiology 15:19–29.
98. Shih, P.M., L.M. Ward, and W.W. Fischer. 2017. Evolution of the 3-hydroxypropionate bicycle and recent transfer of anoxygenic photosynthesis into the Chloroflexi. Proc. Natl. Acad. Sci. U.S.A. 114:10749–10754.
99. Sieber, C.M., A.J. Probst, A. Sharrar, B.C. Thomas, M. Hess, S.G. Tringe, and J.F. Banfield. 2018. Recovery of genomes from metagenomes via a dereplication, aggregation and scoring strategy. Nat. Microbiol. 3:836–843.
100. Simpson, E.H. 1949. Measurement of diversity. Nature 63:688.
101. Singer, E., D. Emerson, E.A. Webb, *et al.* 2011. Mariprofundus ferrooxydans PV-1 the first genome of a marine Fe (II) oxidizing Zetaproteobacterium. PLoS One 6:e25386.
102. Sleep, N.H., and D.K. Bird. 2007. Niches of the pre-photosynthetic biosphere and geologic preservation of Earth's earliest ecology. Geobiology 5:101–117.
103. Søndergaard, D., C.N. Pedersen, and C. Greening. 2016. HydDB: a web tool for hydrogenase classification and analysis. Sci. Rep. 6:34212.
104. Sorokin, D.Y., S. Lücker, D. Vejmelkova, *et al.* 2012. Nitrification expanded: discovery, physiology and genomics of a nitrite-oxidizing bacterium from the phylum Chloroflexi. ISME J. 6:2245.
105. Spear, J.R., J.J. Walker, T.M. McCollom, and N.R. Pace. 2005. Hydrogen and bioenergetics in the Yellowstone geothermal ecosystem. Proc. Natl. Acad. Sci. U.S.A. 102:2555–2560.
106. Stamatakis, A. 2014. RAxML version 8: a tool for phylogenetic analysis and post-analysis of large phylogenies. Bioinformatics 30:1312–1313.
107. Stamenković, V., L.M. Ward, M. Mischna, and W.W. Fischer. 2018. O 2 solubility in Martian near-surface environments and implications for aerobic life. Nat. Geosci. 11:905–909.
108. Stamenković, V., L.W. Beegle, K. Zacny, *et al.* 2019. The next frontier for planetary and human exploration. Nat. Astron. 3:116–120.
109. Stein, L.Y., and M.G. Klotz. 2016. The nitrogen cycle. Curr. Biol. 26:R94–R98.
110. Stookey, L.L. 1970. Ferrozine—a new spectrophotometric reagent for iron. Anal. Chem. 42:779–781.
111. Strous, M., J.A. Fuerst, E.H. Kramer, S. Logemann, G. Muyzer, K.T. van de Pas-Schoonen, R. Webb, J.G. Kuenen, and M.S. Jetten. 1999. Missing lithotroph identified as new planctomycete. Nature 400:446.
112. Suda, K., A. Gilbert, K. Yamada, N. Yoshida, and Y. Ueno. 2017. Compound–and position–specific carbon isotopic signatures of abiogenic hydrocarbons from on–land serpentinite–hosted Hakuba Happo hot spring in Japan. Geochim. Cosmochim. Acta 206:201–215.
113. Swanner, E.D., A.M. Mloszewska, O.A. Cirpka, R. Schoenberg, K.O. Konhauser, and A. Kappler. 2015. Modulation of oxygen production in Archaean oceans by episodes of Fe (II) toxicity. Nat. Geosci. 8:126–130.
114. Takai, K., and S. Nakagawa. 2014. The family Hydrogenothermaceae, p. 689–699. *In* E. Rosenberg, E.F. Delong, S. Lory, E. Stackebrandt, and F. Thompson (ed.), The Prokaryotes. Springer, Berlin, Heidelberg.
115. Tank, M., V. Thiel, D.M. Ward, and D.A. Bryant. 2017. A panoply of phototrophs: an overview of the thermophilic chlorophototrophs of the microbial mats of alkaline siliceous hot springs in Yellowstone National Park, WY, USA, p. 87–137. *In* M. Tank, V. Thiel, D.M. Ward, and D.A. Bryant (ed.), Modern Topics in the Phototrophic Prokaryotes. Springer International Publishing, New York.
116. Thiel, V., M. Hügler, D.M. Ward, and D.A. Bryant. 2017. The dark side of the mushroom spring microbial mat: life in the shadow of chlorophototrophs. II. Metabolic functions of abundant community members predicted from metagenomic analyses. Front. Microbiol. 8:943.
117. Thiel, V., M. Tank, and D.A. Bryant. 2018. Diversity of chlorophototrophic bacteria revealed in the omics era. Annu. Rev. Plant Biol. 69:21–49.
118. Trembath-Reichert, E., L.M. Ward, S.P. Slotznick, S.L. Bachtel, C. Kerans, J.P. Grotzinger, and W.W. Fischer. 2016. Gene sequencing-based analysis of microbial-mat morphotypes, caicos platform, British West Indies. J. Sediment. Res. 86:629–636.
119. Trouwborst, R.E., A. Johnston, G. Koch, G.W. Luther III, and B.K. Pierson. 2007. Biogeochemistry of Fe (II) oxidation in a photosynthetic microbial mat: implications for Precambrian Fe (II) oxidation. Geochim. Cosmochim. Acta 71:4629–4643.
120. Walker, J.C. and P. Brimblecombe. 1985. Iron and sulfur in the pre-biologic ocean. Precambrian Res. 28:205–222.
121. Wang, Q., G.M. Garrity, J.M. Tiedje, and J.R. Cole. 2007. Naive Bayesian classifier for rapid assignment of rRNA sequences into the new bacterial taxonomy. Appl. Environ. Microbiol. 73:5261–5267.
122. Ward, L.M., J. Hemp, L.A. Pace, and W.W. Fischer. 2015. Draft genome sequence of Herpetosiphon geysericola GC-42, a nonphototrophic member of the Chloroflexi class Chloroflexia. Genome Announc. 3:e01352-15.
123. Ward, L.M., J. Hemp, L.A. Pace, and W.W. Fischer. 2015. Draft genome sequence of Leptolinea tardivitalis YMTK-2, a mesophilic anaerobe from the Chloroflexi class Anaerolineae. Genome Announc. 3:e01356-15.
124. Ward, L.M., J.L. Kirschvink, and W.W. Fischer. 2016. Timescales of oxygenation following the evolution of oxygenic photosynthesis. Origins Life Evol. Biospheres 46:51–65.
125. Ward, L.M., S.E. McGlynn, and W.W. Fischer. 2017. Draft genome sequences of a novel lineage of armatimonadetes recovered from Japanese hot springs. Genome Announc. 5:e00820-17.
126. Ward, L.M., A. Idei, S. Terajima, T. Kakegawa, W.W. Fischer, and S.E. McGlynn. 2017. Microbial diversity and iron oxidation at Okuoku—hachikurou Onsen, a Japanese hot spring analog of Precambrian iron formations. Geobiology 15:817–835.
127. Ward, L.M., J. Hemp, P.M. Shih, S.E. McGlynn, and W.W. Fischer. 2018. Evolution of phototrophy in the Chloroflexi phylum driven by horizontal gene transfer. Front. Microbiol. 9:260.
128. Ward, L.M., S.E. McGlynn, and W.W. Fischer. 2018. Draft genome sequence of a divergent anaerobic member of the chloroflexi class ardenticatenia from a sulfidic hot spring. Genome Announc. 6:e00571-18.
129. Ward, L.M., S.E. McGlynn, and W.W. Fischer. 2018. Draft genome sequences of two basal members of the anaerolineae class of chloroflexi from a sulfidic hot spring. Genome Announc. 6:e00570-18.
130. Ward, L.M., P.M. Shih, and W.W. Fischer. 2018. MetaPOAP: Presence or absence of metabolic pathways in metagenome-assembled genomes. Bioinformatics 34:4284–4286.
131. Ward, L.M., B. Rasmussen, and W.W. Fischer. 2019. Primary productivity was limited by electron donors prior to the advent of oxygenic photosynthesis. J. Geophys. Res.: Biogeosci. 124:211–226.
132. Ward, L.M., V. Stamenković, K. Hand, and W.W. Fischer. 2019. Follow the oxygen: Comparative histories of planetary oxygenation and opportunities for aerobic life. Astrobiology 19:811–824.
133. Ward, L.M., and P.M. Shih. 2019. The evolution and productivity of carbon fixation pathways in response to changes in oxygen concentration over geological time. Free Radical Biol. Med. https://doi.org/10.1016/j.freeradbiomed.2019.01.049
134. Waterhouse, A.M., J.B. Procter, D.M. Martin, M. Clamp, and G.J. Barton. 2009. Jalview Version 2—a multiple sequence alignment editor and analysis workbench. Bioinformatics 25:1189–1191.
135. Wickham, H. 2010. ggplot2: elegant graphics for data analysis. J. Stat. Softw. 35:65–88.
136. Wu, Y.W., Y.H. Tang, S.G. Tringe, B.A. Simmons, and S.W. Singer. 2014. MaxBin: an automated binning method to recover individual genomes from metagenomes using an expectation-maximization algorithm. Microbiome 2:26.
137. Yamada, T., and Y. Sekiguchi. 2009. Cultivation of uncultured chloroflexi subphyla: significance and ecophysiology of formerly uncultured Chloroflexi 'subphylum I' with natural and biotechnological relevance. Microbes Environ. 24:205–216.